Supporting Information

Tough and Durable Hydrogels with Robust Skin Layers Formed via Soaking Treatment

*Guoqiang Guo,[a] Yuanzhou Chen,[a] Xiaoyu Liu,[a] Dong Yu Zhu,[a] Bo Zhang,[b] Nengming Lin,[b] Liang Gao[a]**

G. Guo, Y. Chen, X. Liu, Dr. D. Zhu, Dr. L. Gao
[a] School of Chemical Engineering and Light Industry, Guangdong University of Technology, Guangzhou, 510006, China
[*]E-mail: gaoliang@gdut.edu.cn

Dr. B. Zhang, Dr. N. Lin,
[b] Affiliated Hangzhou First People's Hospital, Zhejiang University, School of Medicine, Hangzhou, 310058, China

S1. Materials

Polyvinyl alcohol (PVA) (M_w=146,000-168,000, 98%) are purchased from Sigma-Aldrich. A series of silicates (sodium silicate (SS, also known as water glass in industry) with modules of 3.3 (mole ratio of SiO_2/Na_2O is about 3.3) is ordered from Energy Chemicals (Shenzhen, China). All the reagents are used as received. Deionized (DI) water is used for all experiments.

S2. Synthesis

In a typical synthesis, 1g (~0.023 mol) PVA is dissolved in 10g DI water by vigorous stirring at 90 ^oC for at least 10 h. According to the work pioneered by Peppas,[1] we adopt freezing/thawing treatment to convert the PVA solution into hydrogel. Typically, the PVA solution is cooled to -65 ^oC for 45 min and thawed at 21 ^oC for 6 h. This procedure is conducted only one time to produce a weak PVA hydrogel. The preformed PVA is soaked in largely excessive amount of 40 wt.% SS aqueous solution for n hour at T ^oC. It is assumed that the SS concentration in the liquid phase outside the gel sample remain constant (infinite bath). Then, the as-obtained gels are immersed in large amount of DI water for 7 days until no obvious re-swelling occurs as confirmed by monitoring changes on mass of the gels (**Figure S1)**. The produced hydrogel is referred as PVA-T-n, where T is the soaking temperature in unit of ^oC, and n stands for the soaking duration in unit of hour. During the equilibration, loosely attached SS is removed as indicated by the increased pH value (**Figure S1)**.

SS is produced on an industrial scale with extremely low price. Food and Drug Administration (FDA) has approved SS to be used an antimicrobial rinse, indicating its safety to human. [2] The consumed SS solution after long-term usage can be conveniently regenerated by re-feeding SS powder. PVA has been commercially employed in medical and pharmaceutical coatings, and FDA approved the utilization of PVA in several in vivo tests. [3] Thus, the produced hydrogel can be expected to biocompatible. The whole synthesis process does not produce any waste disposal. No UV radiation and organic solvents are involved. We therefore regard our strategy characters as a low-cost, non-toxic and environment-friendly process. To highlight the unique advantages of sodium silicate, Na_2SO_4 solution, NaOH solution and Na_2SO_4/NaOH mixed solution is also used to treat PVA (90 ^oC for 12 h). The resultant hydrogels, PVA-90-12(Na_2SO_4), PVA-90-12 (NaOH) and PVA-90-12(Na_2SO_4/NaOH) can work as control sets and exhibit much weaker mechanical strength than that of PVA-90-12 (**Table 1**).

S3. Physical Characterizations

Tensile and compressive tests:

Tensile and compressive tests are performed on a Zhuhai SANS (CMT2203) machine at 20 ^oC under a relative humidity of 60%-70%. For tensile tests, rectangular samples with a length of 20 mm, width of 10 mm and thickness of 0.96 mm are tested at a tensile rate of 100 mm

min^{-1}. For compressive tests, cylindrical samples with a diameter of 5 mm and a height of 4.5 mm are tested at a compressive rate of 10 mm min^{-1}. The nominal tensile stress(σ), nominal tensile strain(ε), elastic modulus(E), work of extension (U) and fracture energy (Γ) are obtained from the stress-strain curves. The σ is calculated by dividing the force (F) by the cross-sectional area, and the ε is obtained by dividing stretched length by the original length. The elastic modulus is calculated from the slope over 5-15% elongation in the stress-strain curves. The work of extension (U) is calculated by integrating the area of stress-strain curves (**Equation S1**) according to the literature.

$$U(\varepsilon) = \int_0^{\varepsilon} \sigma d\varepsilon \qquad \textbf{Equation S1}.$$

Fracture energy measurement:

The fracture energy is measured by both classical single edge crack [4] and tearing test [5].

For single edge crack testing, two identical samples with length of 20 mm, width of 10 mm and thickness of 0.96 mm for tensile testing are used. A notch with length of 4 mm along the width is introduced by a razor blade cutting into one of these two samples, with A as the area of cross section of the unnotched sample and L_0 as the initial distance between the clamps. The dimension of the samples is unlikely critical for determination of the fracture energy. [6] A force-extension curve is measured for both the notched sample and an unnotched sample with the same initial dimensions. ΔL_c is defined as the critical extension where the crack propagation starts, and $U(\Delta L_c)$ is the work of extension to reach ΔL_c extension (calculated as

the integral of the force-extension curve). The fracture energy based on single edge crack method is given by:

$\Gamma_{notch} = U(\Delta L_c)/A$ **Equation S2.**

For tearing test, a sample for tensile testing with an initial notch length of 8 mm along the length. The two arms of the hydrogel are clamped. Then, the notched sample is stretched at a 100 mm min^{-1} of tensile rate until the crack propagating through the entire sample. The tearing force (F) at propagation is recorded. The tearing fracture energy is calculated according to equation:

$\Gamma_{tear} = 2F/l$ **Equation S3**.

where l is the thickness of sample.

Water content determination:

Water content of the hydrogels can be calculated by

$$W_{H_2O} = \frac{W_W - W_d}{W_W} \times 100\%$$ **Equation S4**

Where W_w and W_d are the weight of the hydrogel before and after drying at 120 ^oC for 24 h in vacuum.

All mechanical properties and water content are measured for at least three times to produce values with statistics significance.

Structure characterizations:

To clearly characterize the structural and bonding information, the cover and center layer of a thick PVA-90-12 (~4.3 mm) are carefully separated with the aid of sharp razor blade and nail file under photomicroscope.

X-ray diffraction (XRD) is conducted on D8 ADVANCE at a scanning rate of 1°/min on the wet samples. The inset number indicates the degree of crystallinity, which is calculated by **Equation S5**:

$$Degree\ of\ Crystalinity(DC) = \frac{A_1}{A_{total}} \times 100\% \qquad \textbf{Equation S5}$$

where A_1 is the integrated are of XRD peak at 2theta=19.4°; A_{total} is the integrated area under the curve of XRD patterns.

Fourier Transform Infrared Spectra (FTIR) are performed on Nicolet6700 with Attenuated Total Reflection (ATR) accessory (resolution: 4 cm^{-1}) in a glove box filled with dry Ar.

Thermogravimetric analyses (TGA) are performed on a Mettler-Toledo TGA/SDTA851 instrument and recorded at a ramp rate of 10 °C min^{-1} up to 1000 °C under O_2 flow.

Different scanning calorimetry (DSC) is performed on Mettler-Toledo DSC3 under N_2 at a ramp rate of rate of 5 °C min^{-1}.

Scanning electron microscopy (SEM) is conducted on a Hitachi SU8220. The sample is fractured in liquid nitrogen, and the freshly exposed cross section is examined.

Liquid-state ^1H NMR experiments are carried out on a Bruker 400M spectrometer. DMSO-d_6 is used as a solvent. PVA-90-12 can be dissolved in DMSO at 90 °C.

S4. Cytotoxicity assay

RAW264.7 is obtained from the Cell Bank of the China Science Academy (Shanghai, China). The cell line has been tested and authenticated utilizing short tandem repeat (STR) profiling every 6 months. RAW 264.7 is cultured in DMEM contained 10% FBS and 100U per mL of penicillin-streptomycin in a 5% CO_2 humidified incubator at 37 ^{o}C.

For the analysis of cell proliferation, RAW264.7 cells are seeded in 6-well plates in a density of 5×10^5/well, and subsequently treated with indicated concentrations of PVA-90-12 for 72 hours. Viable cells are stained by methylrosanilnium chloride solution and the plates were read on automated microplate spectrophotometer (Thermo Mutiskan Spectrum, Thermo Electron Corporation) at 570 nm. The survival rate of cell proliferation for each well was calculated. To evaluate the biocompatibility of PVA-90-12, RAW264.7 macrophages are used to perform the cytotoxicity test. The sterilized PVA-90-12 were first dissolved in DMSO and then dropped into PBS buffer. The solutions of PVA-90-12 are then added to cells at indicated concentrations.

Table S1. Reported tough hydrogels that can maintain mechanical performance under environmental loads. The PVA-90-12 hydrogel possesses a rare combination of mechanical properties and chemical stability where each individual parameter is parallel to or exceeds those of some of the current best-in-class synthetic hydrogels.

Samples	σ_f (MPa)	ε_f (%)	E (MPa)	Γ (kJ/m^2)	Stability	Reference (published year)
PBMA-*b*-PMAA-*b*-PBMA/PAM	~10	~600	~2	~3	Concentrated saline solution at room temperature	[7] (2016)
PVA-PAM	~2.5	~400	~5	~14	Concentrated saline solution at room temperature	[8] (2014)
PNAGA	~1.1	~1100	~0.15	~1.2	PBS, pH 3-10, at room temperature	[9] (2015)
DHIR60–5–35-d	~8.3	~700	~5.61	~5.5	PBS, at room temperature	[10] (2015)
PVA-ANF	~5		~9.1	~9	PBS at 37 ^{o}C	[26] (2018)
Tretra-armed PEG	~0.2	~800			PBS at 37 ^{o}C	[11] (2014)
PDMS-PNIPAM	~0.05	~950		~1	water at 60 ^{o}C	[12] (2016)
PAM/XG	~1.5	~1050	~0.46		pH=2-10 at room temperature	[13] (2016)
PVA-90-12	~5	~440	~2.4	10-12	60 ^{o}C DI water, PBS, pH=1-14, Urea, NaSCN	This work

There are several impressive precedents that combine high mechanical strength and good stability. Gong's Lab reports a highly stable DN hydrogel constructed through hydrophobic and hydrogen bonding interactions.[7] After equilibrating in water and 3M NaCl solutions for 3 days, this hydrogel still exhibits an ultrahigh fracture stress of ~9 MPa at a fracture strain of ~500-600%. The stability of this hydrogel originates from the water-resistant hydrophobic interaction and the formation of stable hydrogen-bonding pairs. Liu's Lab synthesizes a tough and highly stable supramolecular hydrogel stemming from the formation of abundant dual hydrogel bonds.[9] Tensile strain of 1200%-1500% and strength of ~0.9-1.1 MPa can be retained upon soaking in various medias, including water, PBS, acidic and alkaline. In these above-mentioned examples, good stability is demonstrated under ambient conditions. However, the temperature of psychological condition ranges 37-42 ^{o}C,[14] and the operation conditions for engineering could be even harsher.[15] To endow stability in aqueous solution at elevated temperature, an intriguing method is to incorporate lower critical solution temperature(LCST)-type segments in hydrogel.[11, 16] When the temperature increases, the LCST groups can undergo phase separation from aqueous phase to enhance the hydrophobic interactions. Therefore, the mechanical properties are retained and even improved at elevated temperature. However, such kind of existing systems suffer very low tensile strength (<0.05 MPa).[11, 16]

Table S2. Comparison on the testing state of tough hydrogels that fabricated through soaking strategies. In the literatures, the mechanics of produced hydrogels are only evaluated in the as-prepared state. These hydrogels are catastrophically weakened when being immersed in water. By contrast, the superior mechanics of PVA-90-12 are demonstrated in its fully swollen state.

Hydrogel components	State of sample for mechanical testing	Treatment method [a]	Mechanism	Tensile properties [b]				Reference (published year)
				σ_f (MPa)	ε_f (%)	E_f (MPa)	Γ (kJ/m^2)	
PVA	No equilibration in water	NaCl soaking	Crystallization	1.61	631			[17] (2016)
PAM-CS		NaOH soaking	Crystallization	2	450	0.35	12.5	[18] (2016)
PAM-CS		NaCl soaking	Hydrophobic interaction	1.9	600	0.3	8	[18] (2016)
Gelatin		$(NH_4)_2SO_4$ soaking	Hydrophobic and H-bonded interaction	4.3	528	0.56		[19] (2017)
Polysaccharide		EtOH soaking at 25 ^oC	Multiple Physical crosslinking	2.6-2.7	55-81	4.9-3.2		[20] (2016)
Chitin		EtOH soaking at 25 ^oC	Multiple Physical crosslinking	3.98	81	0.22		[21] (2016)
CS-PAM		Na_2SO_4 soaking at 25 ^oC	Ionic-interaction	3.7	400	0.8	9.8	[22] (2018)
CS-PAM		Na_3Cit soaking	Ionic-interaction	5.6	400	1.3	14	[22] (2018)
PVA-90-12	Fully swollen in water	Sodium silicate soaking at elevated temperature	Crystallization and fluid-dependent viscoelasticity	5	440	2.4	10-12	This work

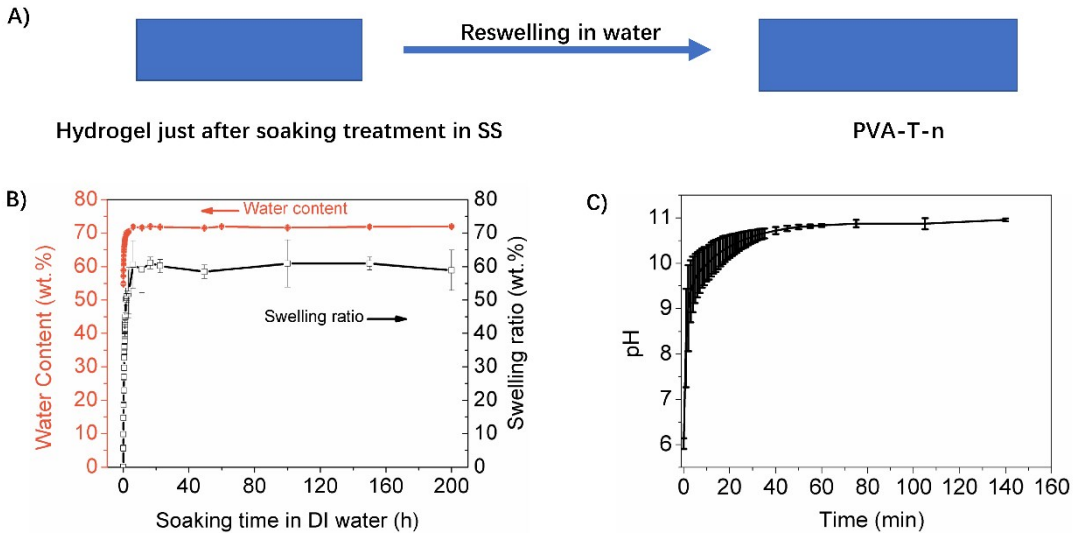

Figure S1. Equilibration of as-soaked hydrogel in D.I water (taking PVA-90-12 as an example): (A) The process of reswelling for the as-soaked hydrogel; (B)water content and swelling ratio of hydrogel; (C) pH increasement during the reswelling process. To monitor the water content and swelling ratio, the as-soaked hydrogel is soaked in infinite water bath, while to monitor the pH changes, 1 g as-prepared hydrogel is immersed in 10 mL DI water so that the changes in pH are sufficiently pronounced to be measured. Clearly, the reswelling process involves water adsorption and removal of residual SS.

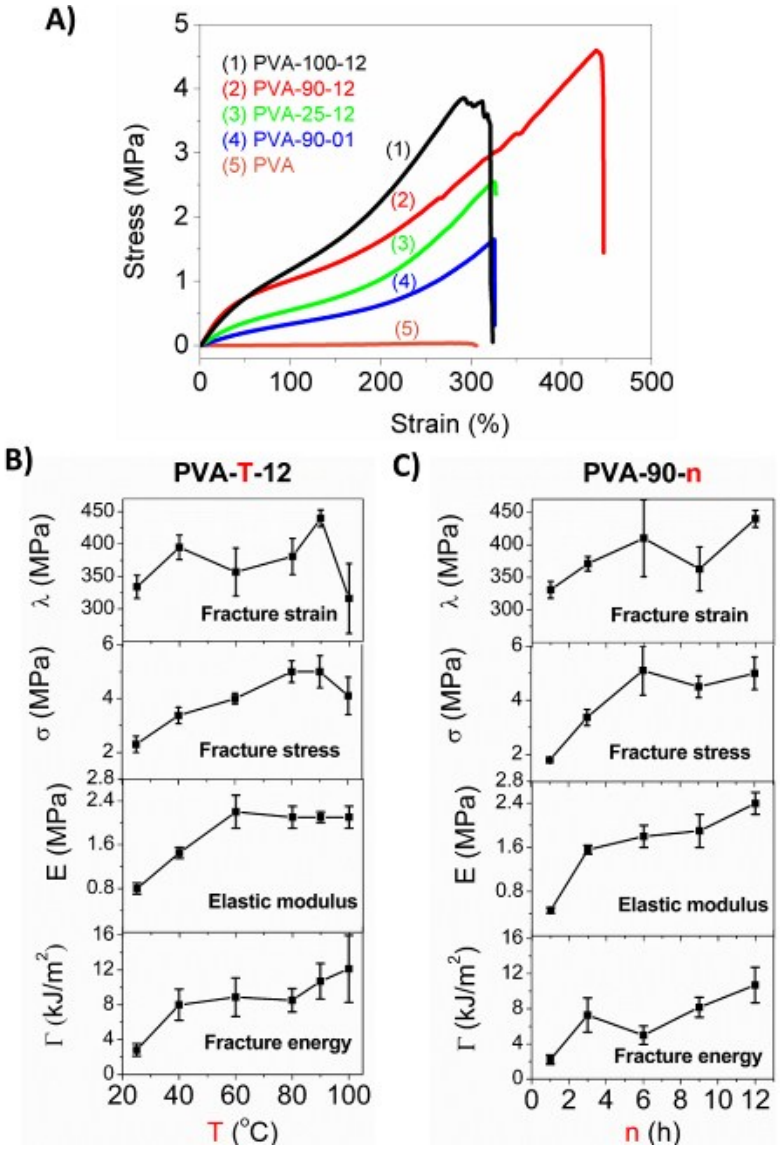

Figure S2. Optimization of mechanical properties through varying the soaking temperature (T) and duration (n). (A) Typical tensile curves of PVA-T-n; mechanical properties of (B) PVA-90-n and (C) PVA-T-12 series. We find that (1) at a given soaking temperature (*e.g.* 90 ^{o}C), prolonging soaking duration can generally strengthen the gels. When the soaking duration is over 12 h, water content decreases to 70%, which is the typical value for natural ligaments; (2) at a given soaking duration (*e.g.* 12 h), increasing soaking temperature enhances stiffness. When the temperature is over 90 ^{o}C, the resultant gel shows increased stiffness, for example, the stress of PVA-100-12 between strains of 100% and 300% is obviously larger than that of PVA-90-12. However, both fracture stress and strain of PVA-100-12 becomes lower than that of PVA-90-12. This result may imply "ductile-to-brittle" transition, [23] which means that there is no sufficient amount of ductile network in the gel to withstand force transferred from the fracture of brittle networks. The imbalance of ductile and brittle components results in stress concentration and rupture under stretching.[24] Therefore, both stress and strain decreases.

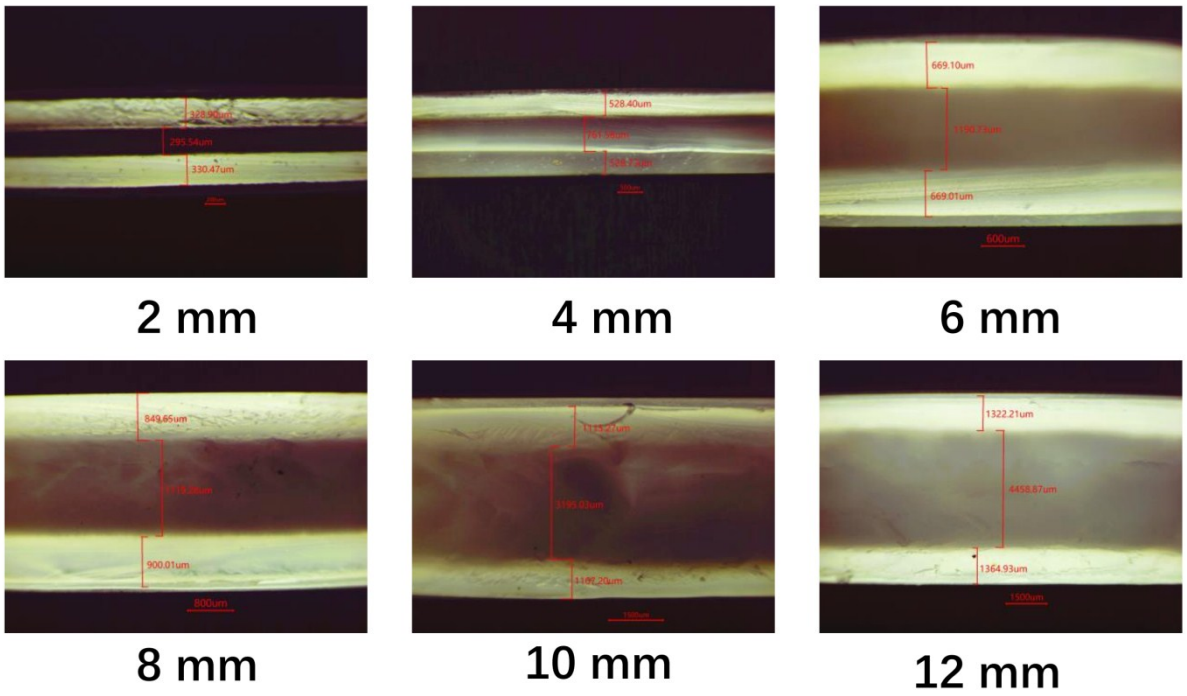

Figure S3. Tunable thickness ratio of cover and center layer: Light microscopy of PVA-90-12 prepared by soaking PVA with different thickness (as indicated below each picture).

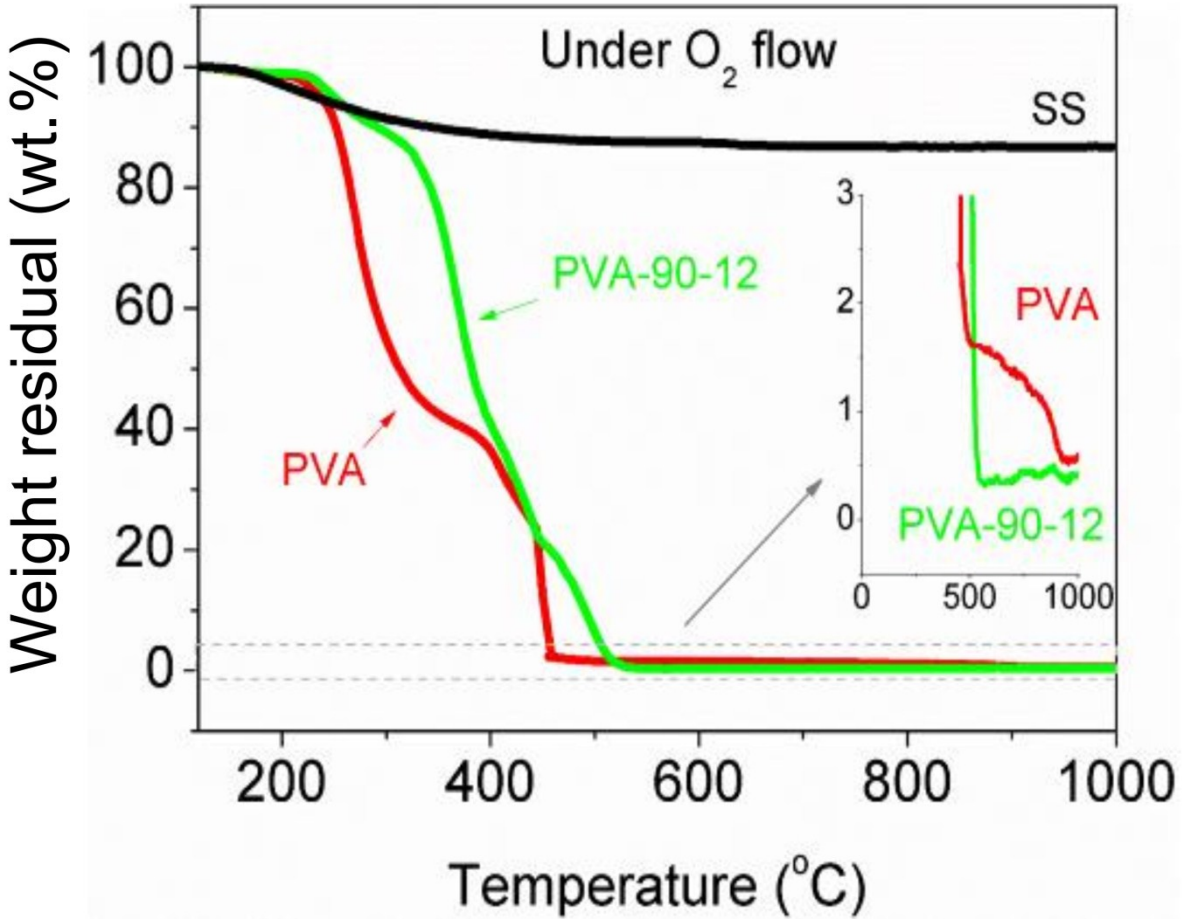

Figure S4. Thermal decomposition of hydrogels: TGA curves of freeze-dried SS, PVA, and PVA-90-12 as indicated in the figure. Ramping rate: 5 °C/min; Flow rate: O_2, 100 mL/min. Before data recording, the samples were heated to 120 °C and kept at this temperature for 1 h to fully remove water. Upon heating to 1000 °C, the weight loss of SS is about 10%, while both PVA and PVA-90-12 exhibits only about 0.5 wt.% residual, which is probably contributed by the impurity of PVA reagent. These results when combined suggest that there is negligible amount of SS in PVA-90-12. If there is certain amount of SS in PVA-90-12, the residual weight percentage should be higher than that of neat PVA. For example, 5 wt.% SS in PVA should produce over 4 wt.% residual, which is sufficiently high to be detected by TGA equipment. In addition, the major thermal decomposition of PVA-90-12 occurs at higher temperature than that of PVA, suggesting higher thermal stability.

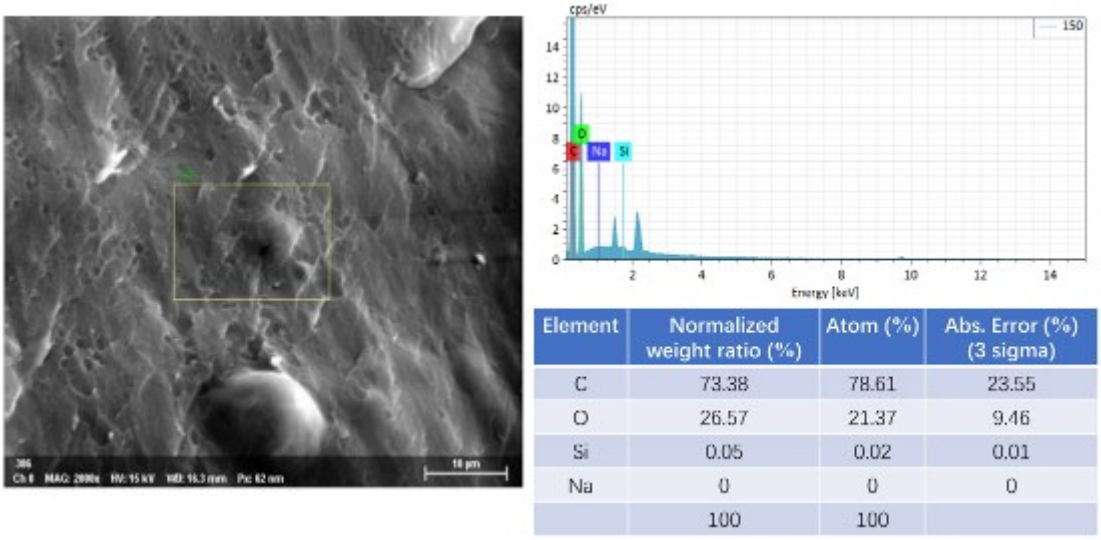

Element	Normalized weight ratio (%)	Atom (%)	Abs. Error (%) (3 sigma)
C	73.38	78.61	23.55
O	26.57	21.37	9.46
Si	0.05	0.02	0.01
Na	0	0	0
	100	100	

Figure S5. Energy dispersion X-ray (EDX) spectra of PVA-90-12. There is no detectable Na atom. When combined with results of FTIR in Figure 4A (main text) and TGA in Figure S4, this result suggests that an overwhelming majority of SS detaches from PVA-90-12 during the equilibration process as illustrated in Figure S1. The trace amount of Si could exist in PVA-90-12 in the formation of SiO_2, which is formed by the reaction between SS and CO_2 in air.

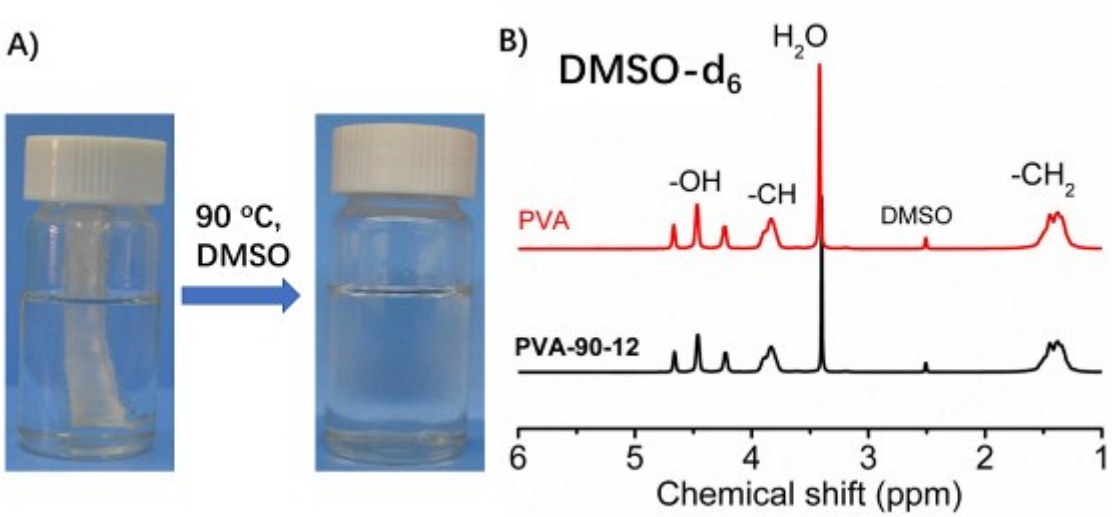

Figure S6. (A)Physical observation of dissolution of PVA-90-12 in DMSO at 90 °C;(B) liquid ^{1}H NMR spectra of PVA powder and PVA-90-12 hydrogel as dissolved in DMSO-d_6. Clearly, the chemical shift of PVA-90-12 is exactly the same to that of the pristine PVA hydrogel, meaning there is no chemical reaction between PVA and SS during the soaking treatment.

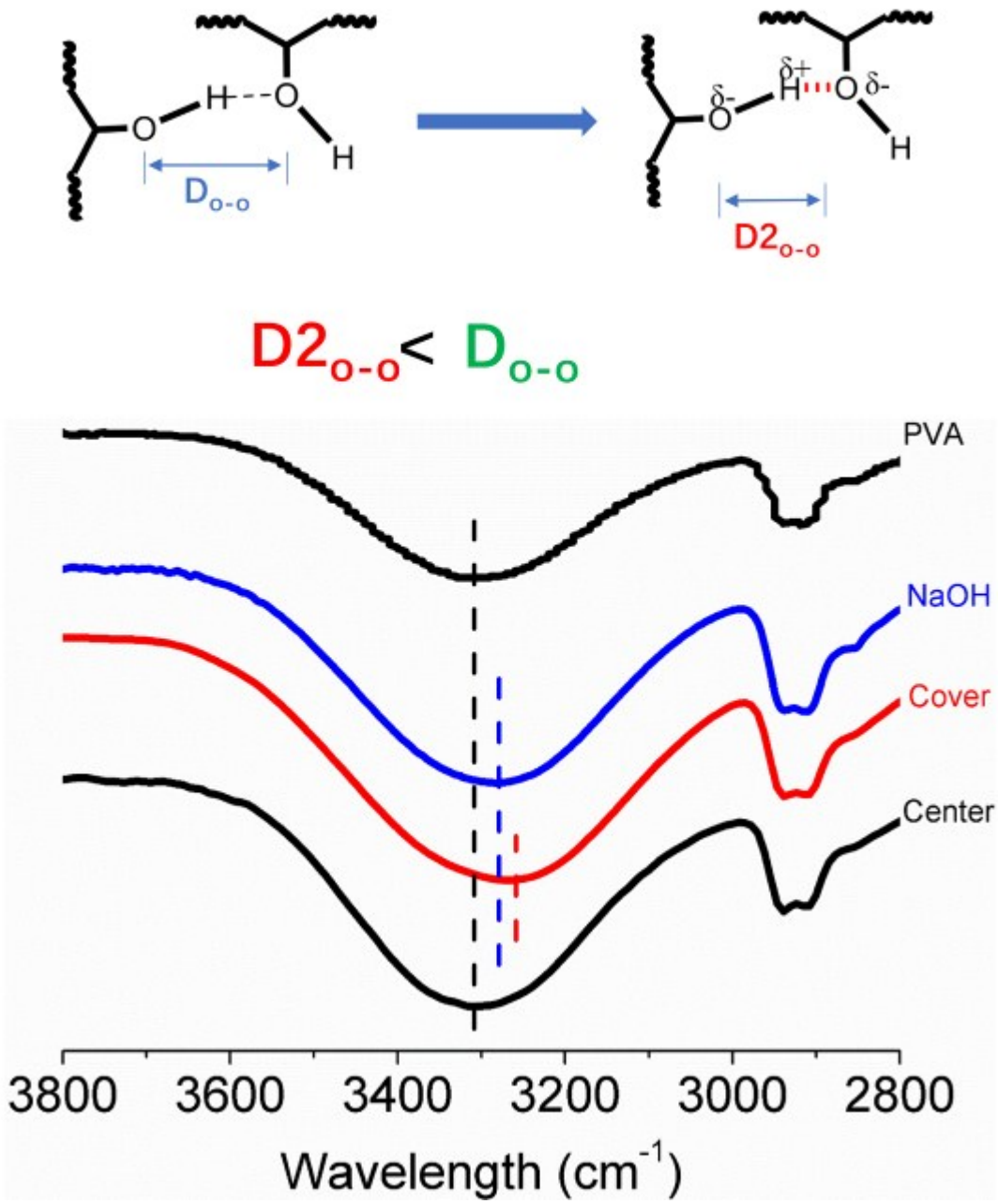

Figure S7. ATR-FTIR spectra of initial PVA gel, PVA-90-12(NaOH) gel treated in NaOH solution (conc. ~1.86 M, 90 ^{o}C, 12 h), cover and center of PVA-90-12. Clearly, in analogue to that of cover in PVA-90-12, the -OH absorption of PVA upon soaking treated in NaOH shows red-shifting, even though the shifting value is slightly smaller than that of SS treated PVA-90-12. Note that although this shifting is small, the results are highly reproducible.

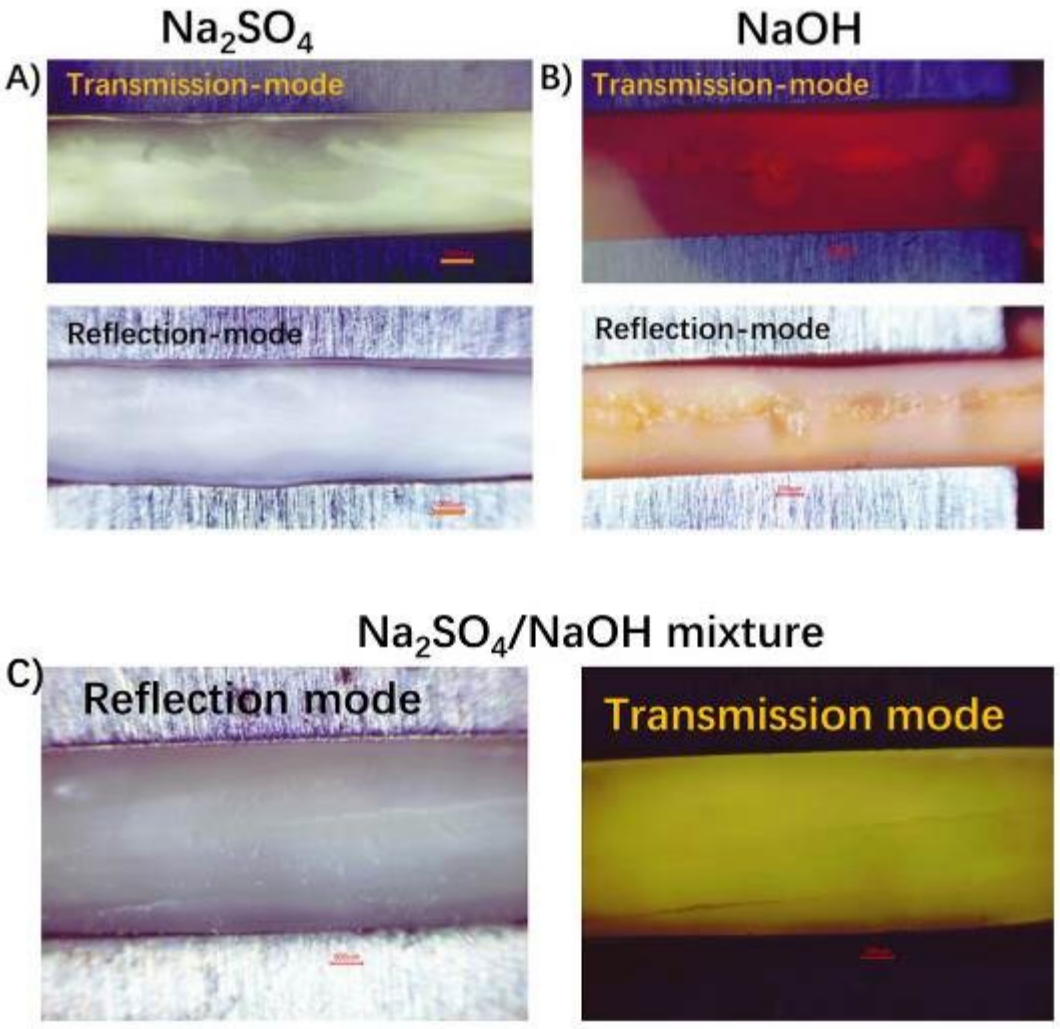

Figure S8. Cross section of (A) Na_2SO_4, (B) NaOH and (C) mixture of Na_2SO_4/NaOH treated PVA hydrogel as observed in optical microscopy under transmission and reflection mode; The treating conditions are exactly same to that of PVA-90-12 as treated by SS. Clearly, there is no layered structure formed. We believe that these salting out and polarization effects must subtly cooperate with each out to create the macroscopic skin layer.

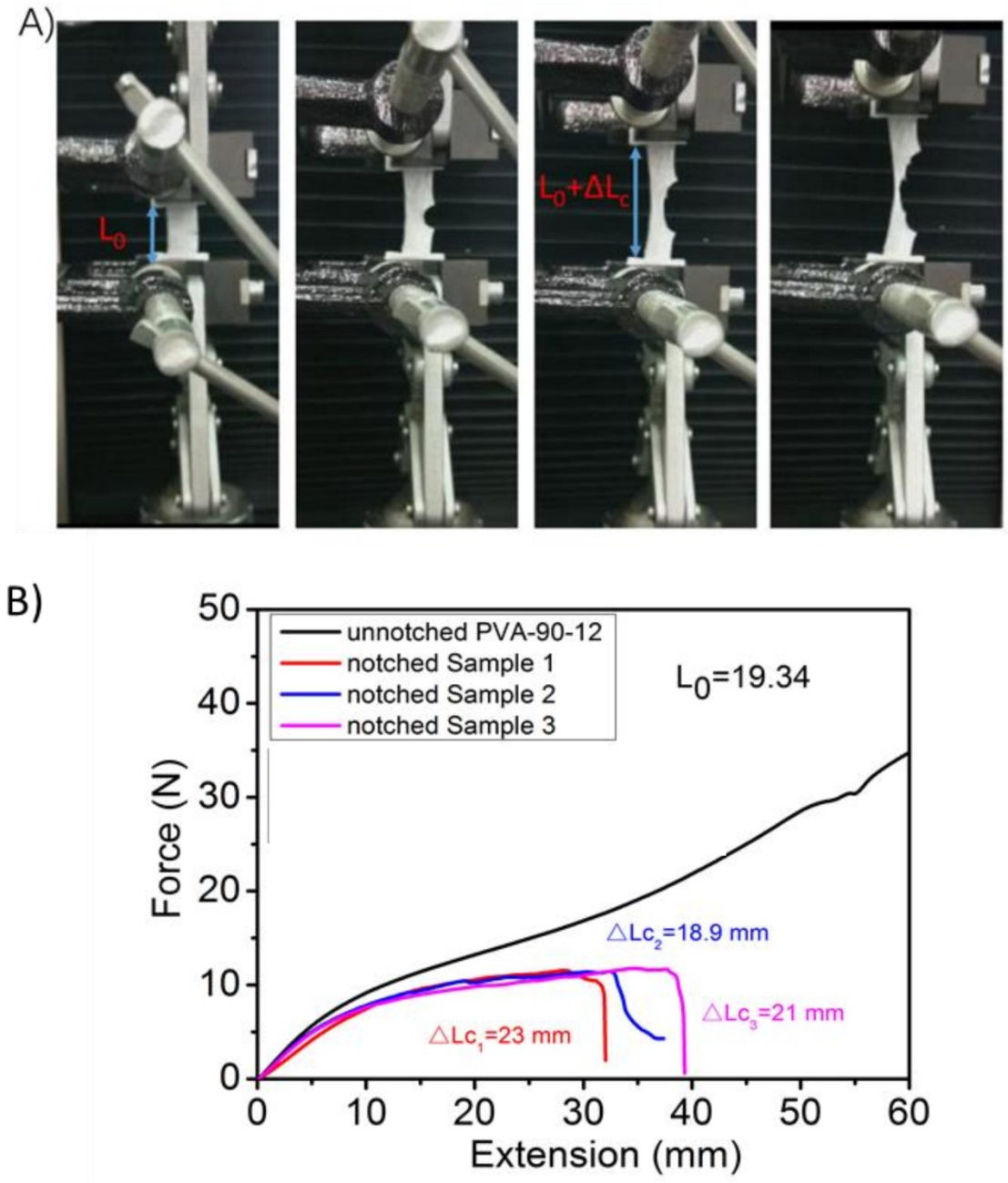

Figure S9. Single edge crack method to determine the fracture energy of PVA-90-12. (A) Physical observation for the stretching; (B) Force-extension curve of notched PVA-90-12 hydrogel. The calculated fracture energy is over10 kJ/m^2 according to **Equation S2**.

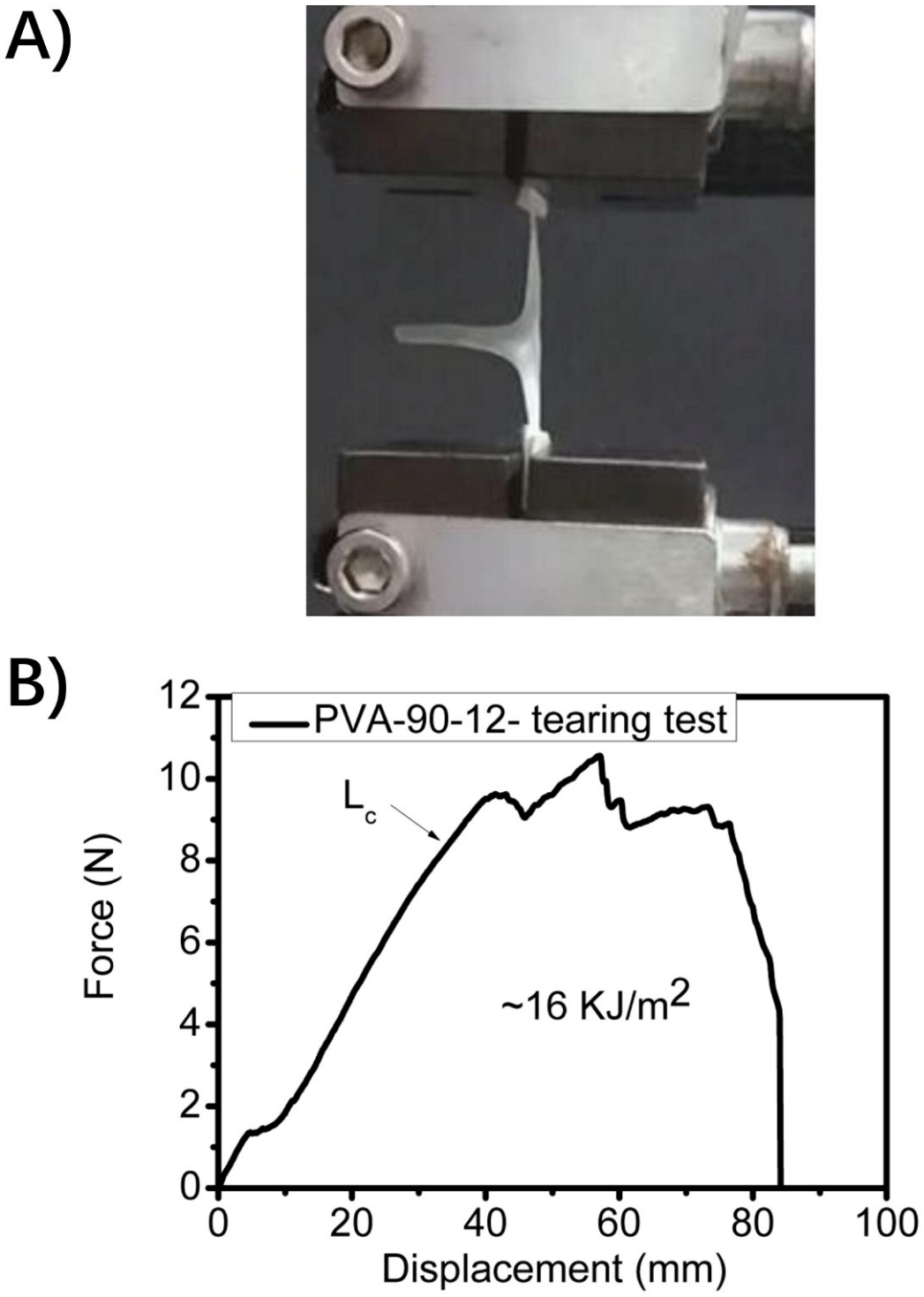

Figure S10. Tearing method to determine the fracture energy of PVA-90-12. The calculated fracture energy is about 12 kJ/m^2 -16 kJ/m^2 according to **Equation S3**. The hydrogel is ruptured from crack, not from the arm.

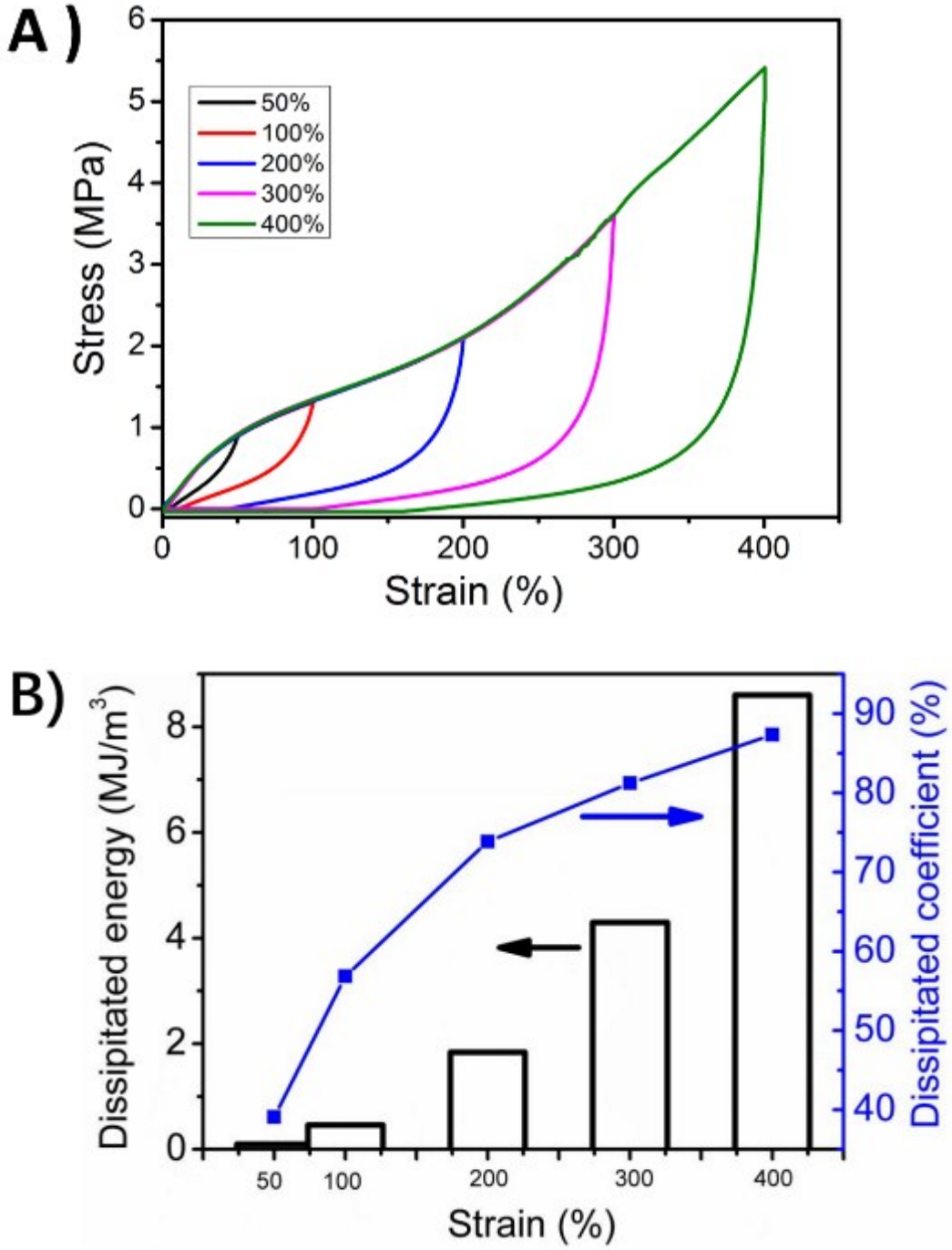

Figure S11. (A) Loading-unloading curves of PVA-90-12 hydrogels under different strains; fresh sample is used for each cyclic testing; (B) The calculated dissipated energy and dissipation coefficient of PVA-90-12 hydrogel during the loading-unloading testing.

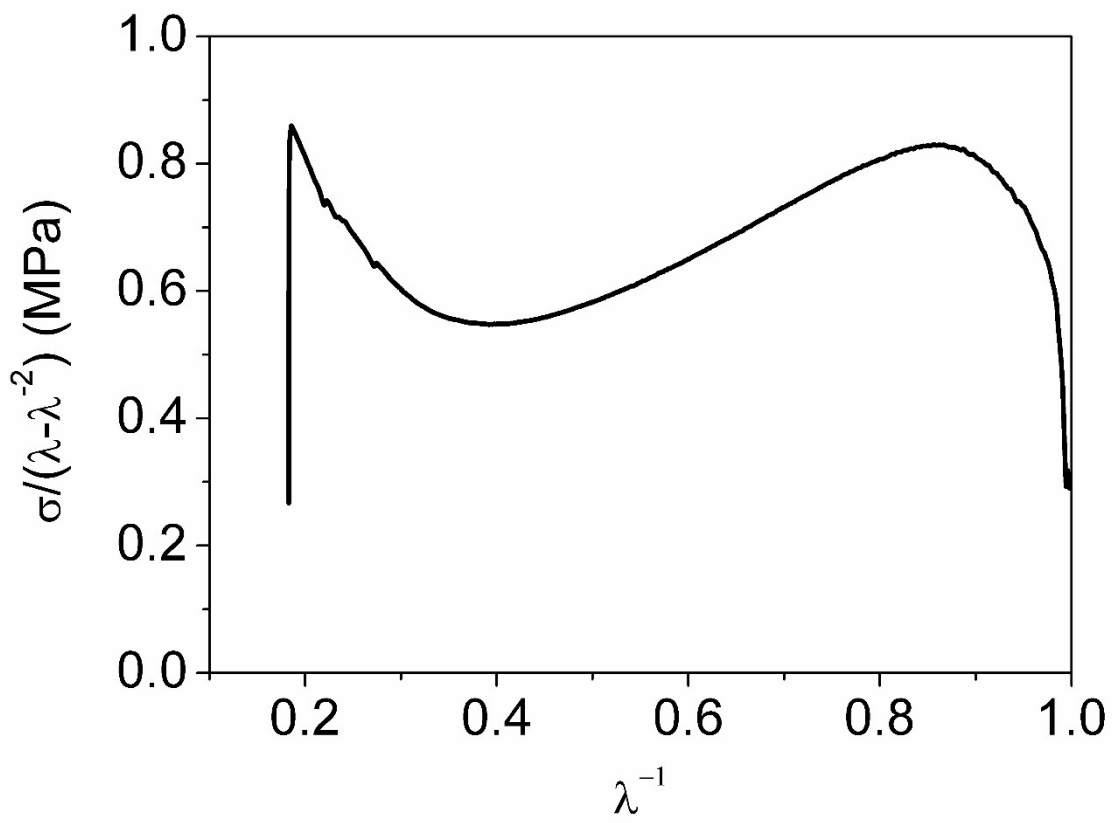

Figure S12. Mooney-Rivlin curves of PVA-90-12. The curve is plotted by analyzing the strain-stress curve of PVA-90-12 according to the phenomenological Mooney-Rivlin equation as follows:

$$\sigma_{red} = \frac{\sigma}{\lambda - \lambda^{-2}} = C_1 + C_2 \frac{1}{\lambda} \qquad \textbf{Equation S6}$$

Wherein σ_{red} is the reduced stress, λ is the extension ratio equal to strain+1, and C_1 and C_2 are material constants. C_1 is related to the shear modulus, while C_2 is indicative of strain softening ($C_2>0$) and strain hardening ($C_2<0$). Clearly, at small strain ($\lambda^{-1}<0.75$), the PVA-90-12 shows distinct strain hardening under deformation. This result suggests that the chains of PVA-90-12 between crystalline crosslinking knots are stretched. At large deformation, the crystalline slippage occurs, resulting in the strain softening.

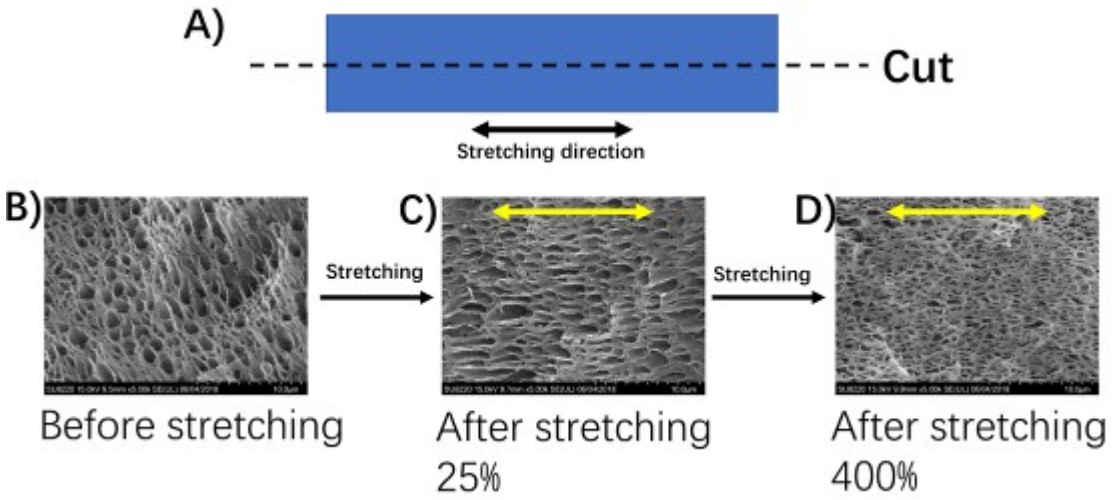

Figure S13. SEM images of the cross section of (B) virgin PVA-90-12 and a relaxed PVA-90-12 sample after (C)one loading-unloading cycle of 25% and (D) 400% tensile strain. The yellow arrow indicates the direction of tension as illustrated in (A). There are negligible changes on the microscopic morphology under small deformation (25%). At large strain (400%), the cavities are distorted, suggesting plastic deformation.

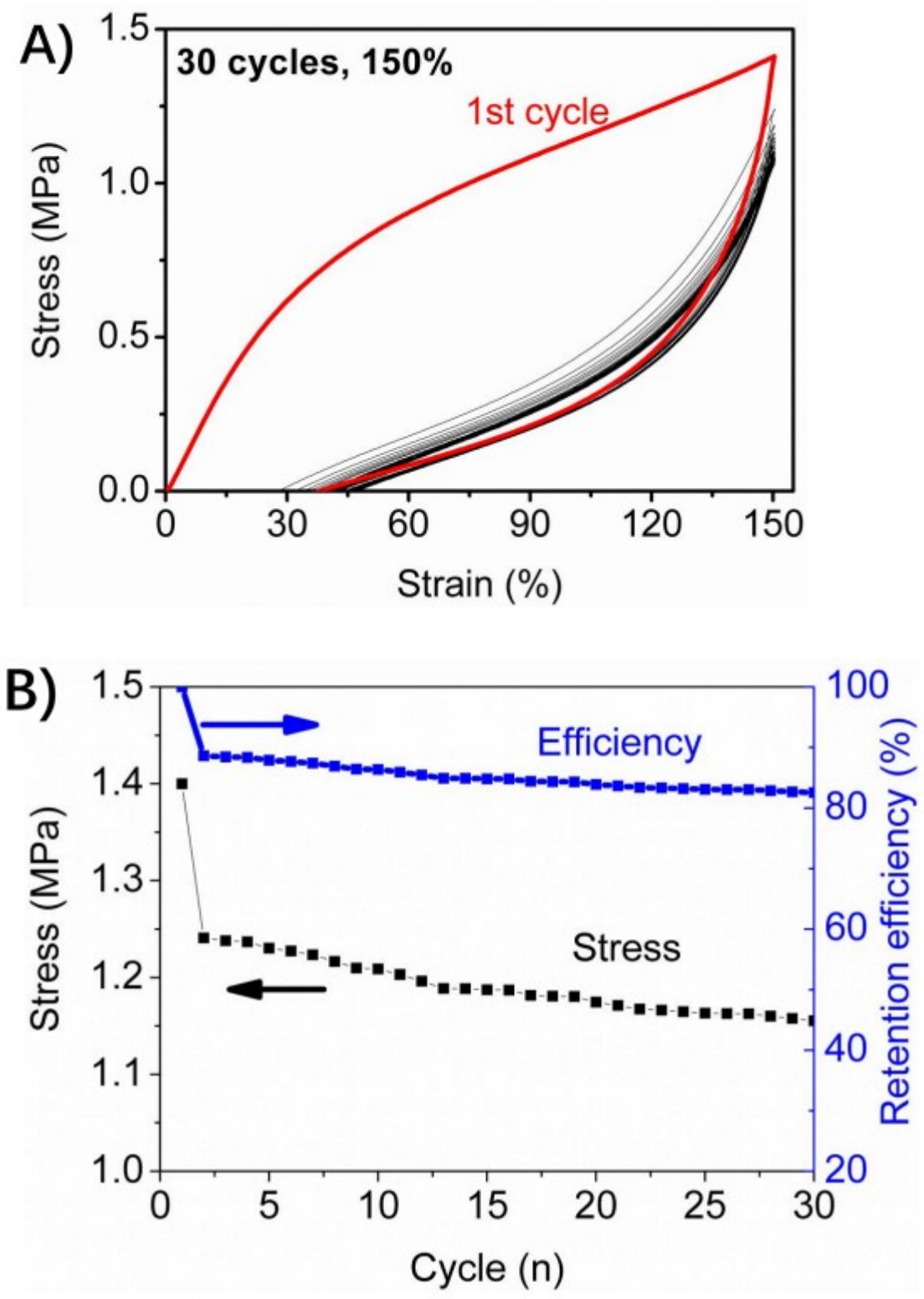

Figure S14. (A) 30 successive loading-unloading cycles of PVA-90-12; (B) The remained maximum stress of PVA-90-12 in 30 continuous loading-unloading cycles.

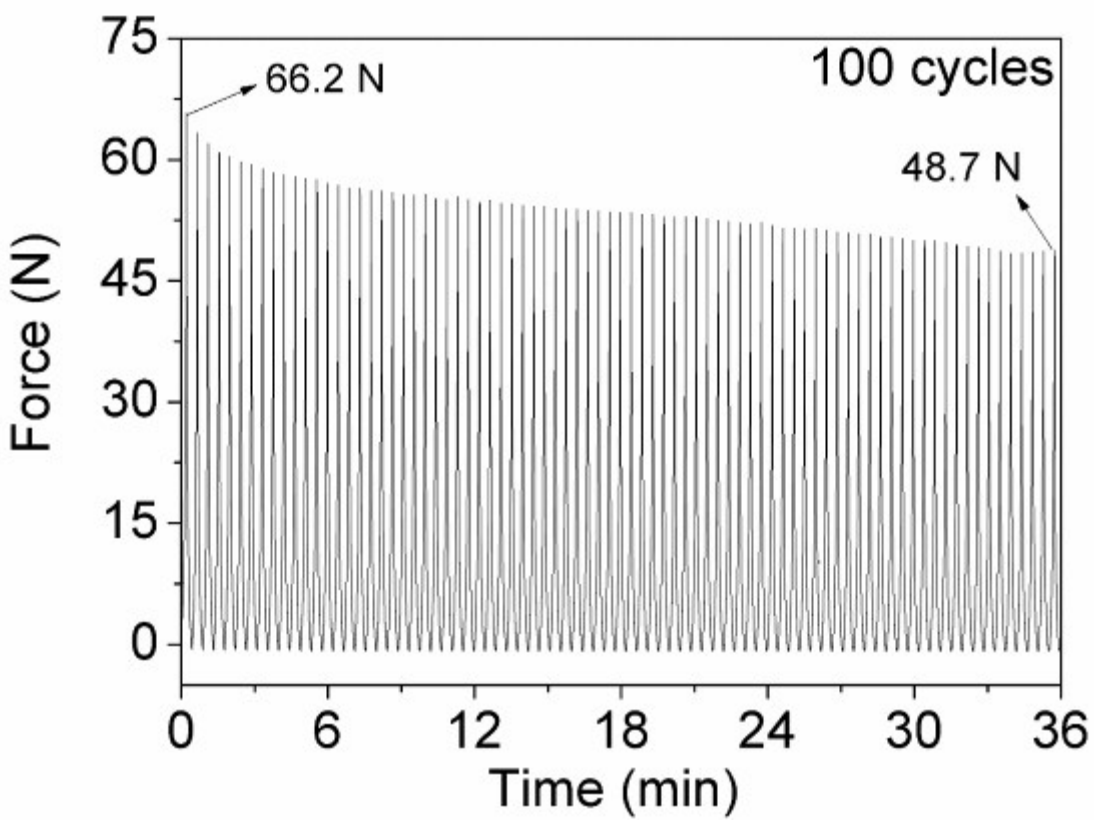

Figure S15. The load-time curve at a fixed compressive strain of 48%. 80 cycles at a rate of 10 mm/min.

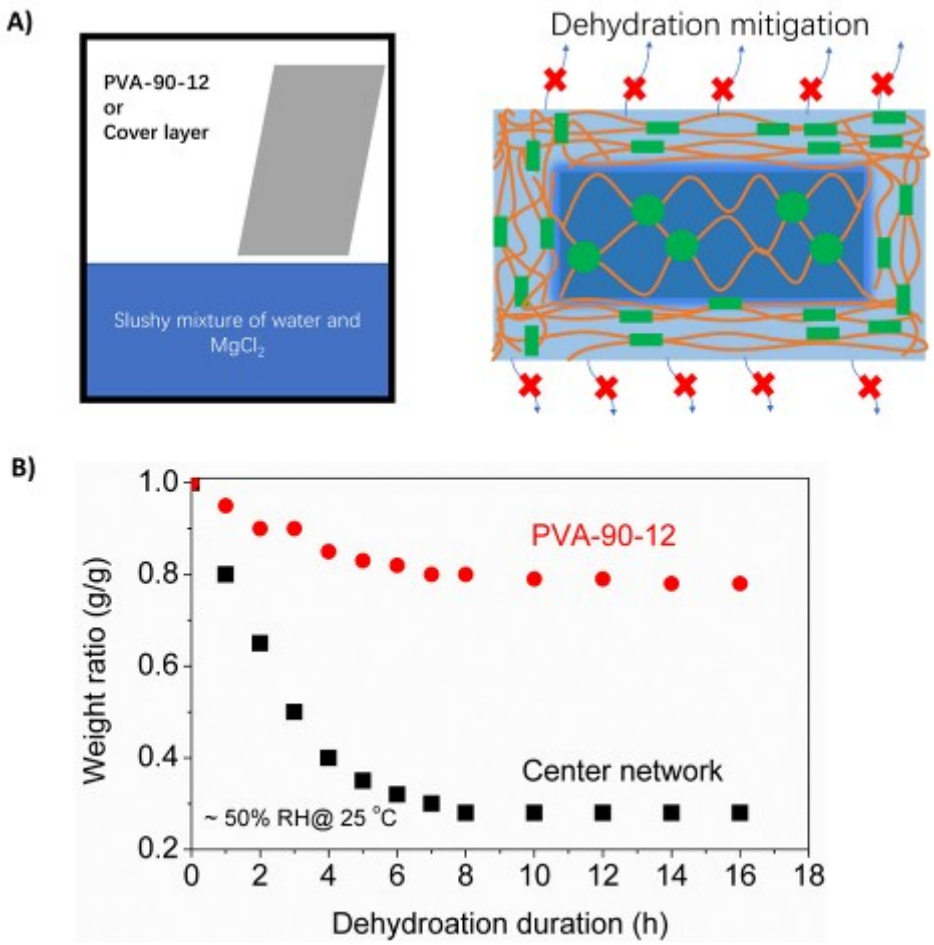

Figure S16. Anti-dehydration of PVA-90-12. (A) Schematic illustration of the humidity chamber and anti-dehydration of PVA-90-12 due to the presence of cover layer; (B) Temporal dehydration of PVA-90-12 and its center layer under a relative humidity of ~40% at 25 ºC. This result imply the essential role of cover layer in suppressing water evaporation perhaps due to its dense structure.

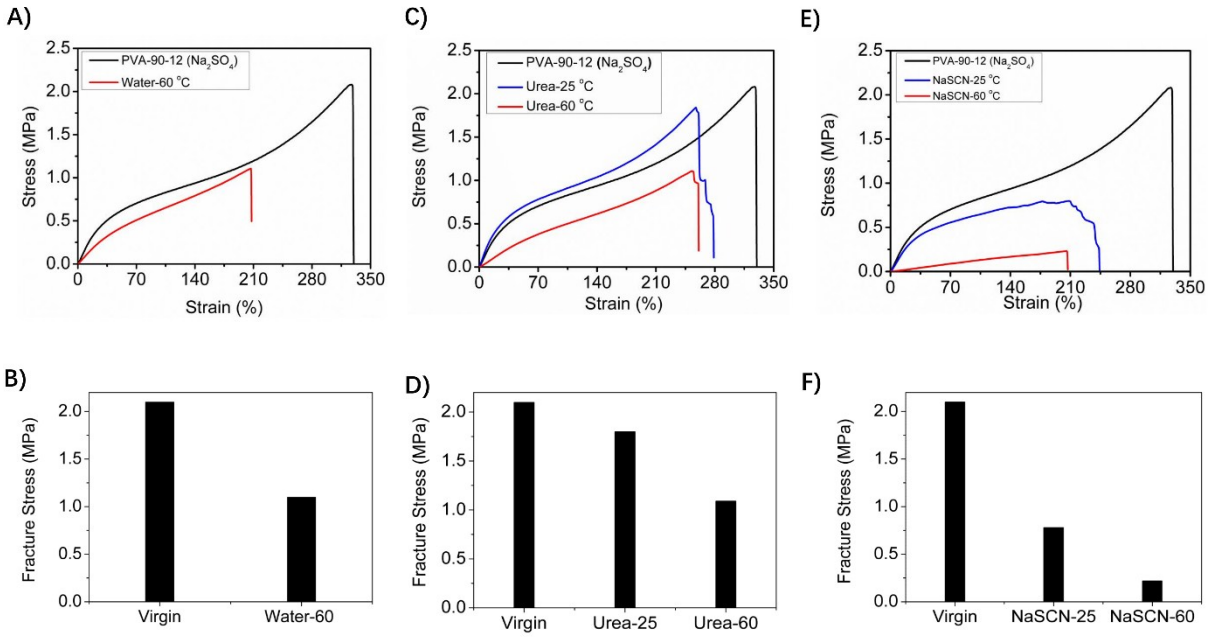

Figure S17. Typical stress-strain curves of Na_2SO_4 treated PVA after being immersed in various aqueous media. Cleary, the stability of PVA-90-12(Na_2SO_4) hydrogels is much lower than that of PVA-90-12. For example, after soaking in NaSCN 60 ^oC for 24 h, the remaining stress of PVA-90-12(Na_2SO_4) is only 0.2 MPa. This is more than ten times lower than that of PVA-90-12. We did not evaluate the stability of PVA-90-12 (NaOH) and PVA-90-12 (NaOH/Na_2SO_4) simply because its mechanical performance is too poor to be applicable as structural materials.

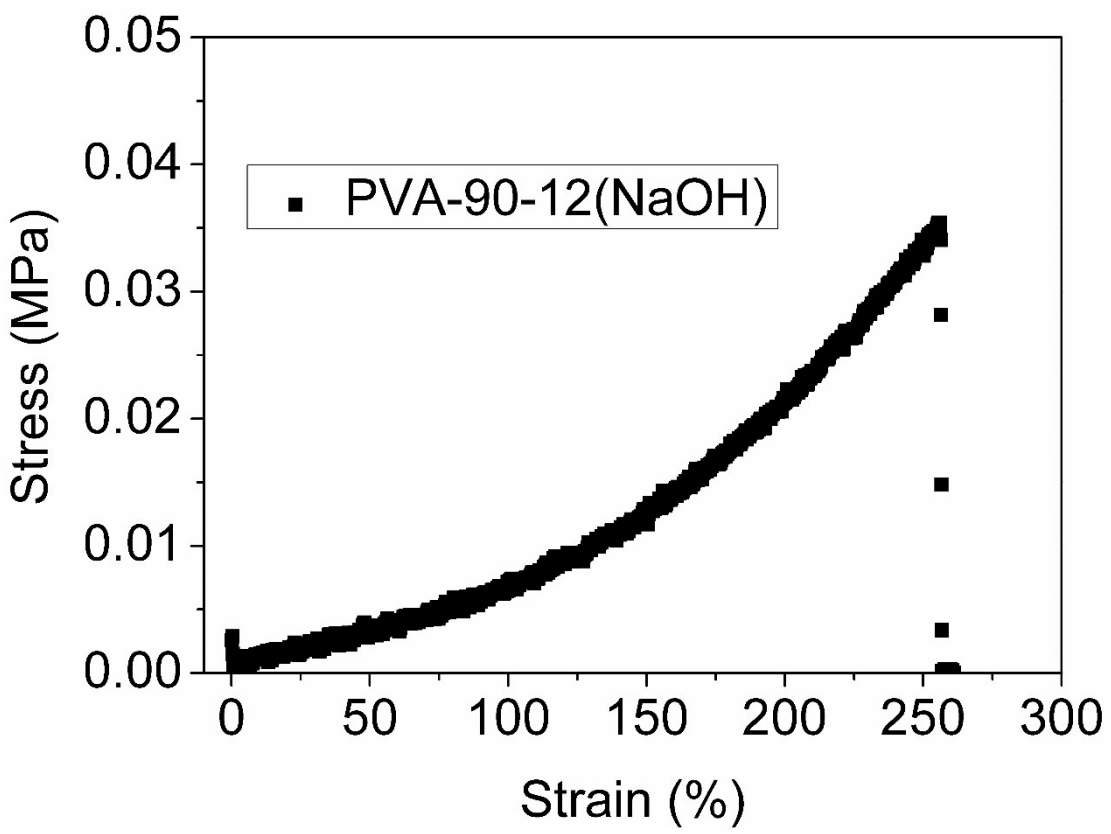

Figure S18. The stress-strain curve of PVA-90-12(NaOH), which is prepared by soaking PVA gel in 1.86 M NaOH solution for 12 h at 90 ^{o}C. PVA-90-12(NaOH) is very weak. The -OH groups are indeed polarized according to FTIR spectra in Figure S7. However, NaOH cannot induce dehydration of PVA hydrogel perhaps because NaOH is not strong salting out reagent. Therefore, there is no crystallites formed in PVA-90-12(NaOH). When the polarized -OH groups are not orderly packed, the intensity of the formed dipole-dipole interaction could be drastically weakened.

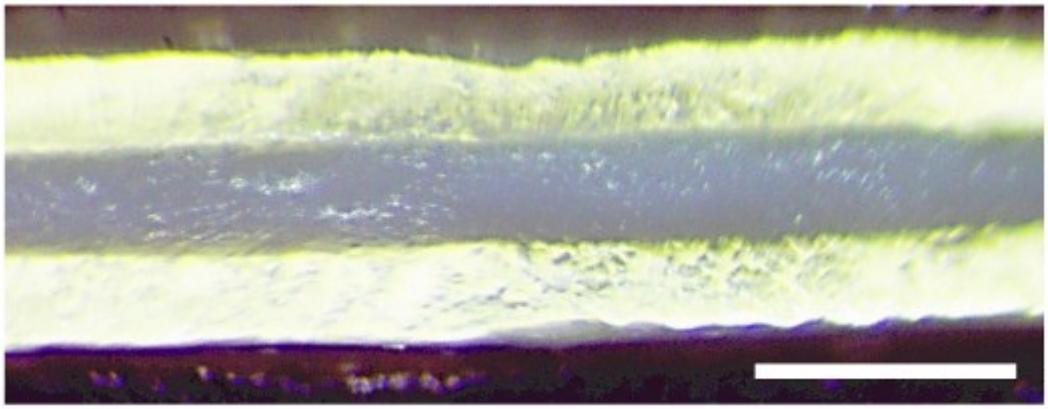

Figure S19. Photomicroscope of PVA-90-12(STPP1.86 M) (reflection mode), which is prepared by soaking PVA in sodium tripolyphosphate solution at 90 ^{o}C for 12 h. The main purpose of this study is to verify our hypothesis that the salts with large ion size can lead to the formation of layered structure. Scale bar: 1 mm.

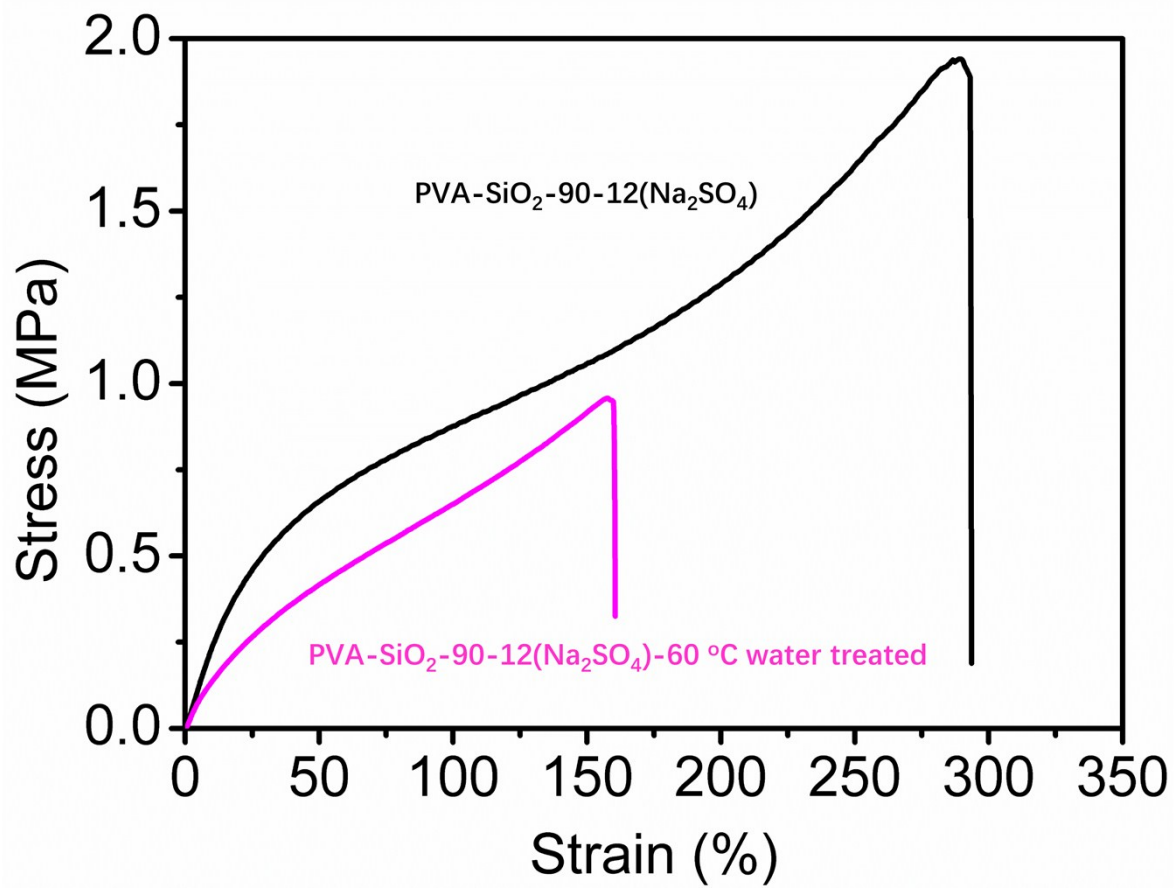

Figure S20. Typical stress-strain curves of Na_2SO_4 treated SiO_2 doped PVA before and after treatment in 60 °C water. Cleary, the stability of PVA-90-12(Na_2SO_4) hydrogels is barely enhanced after SiO_2 doping.

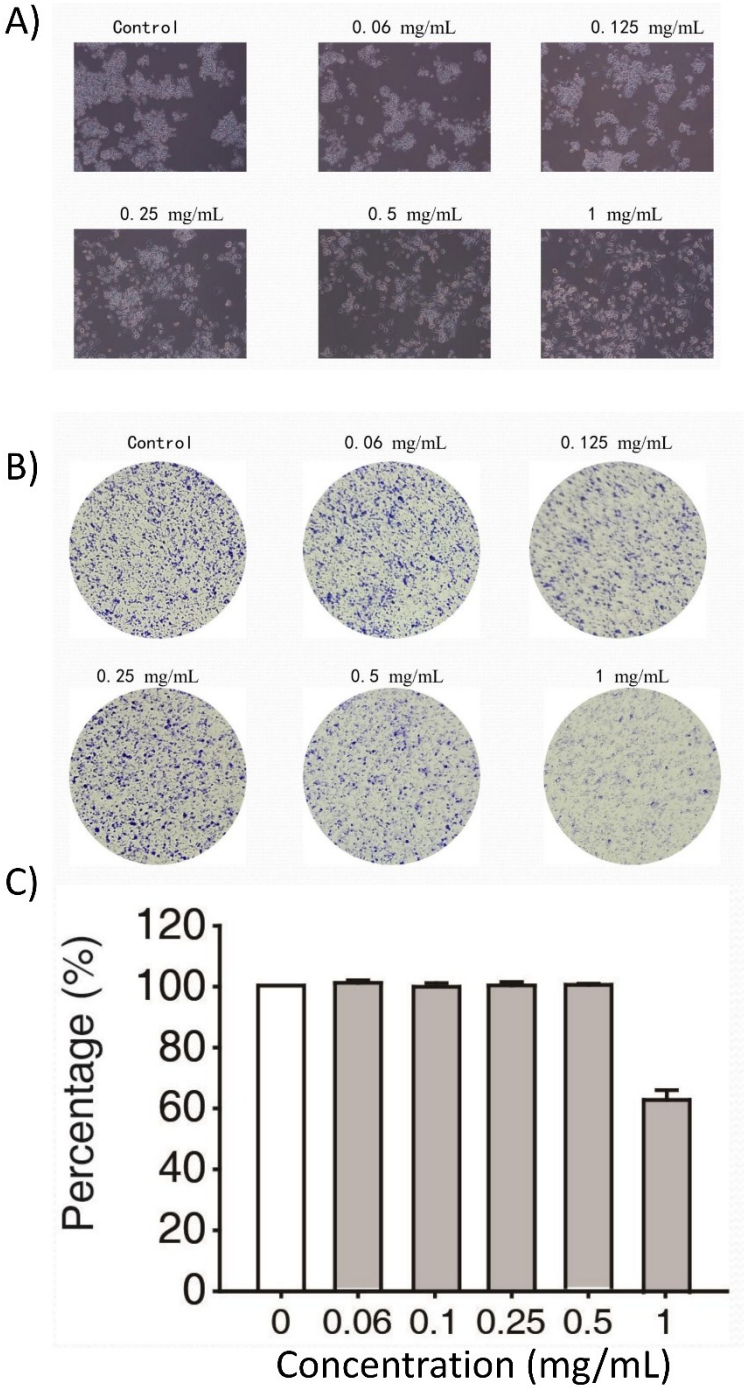

Figure S21. (A) Morphology of RAW 264.7 macrophages after culturing on TCPS for 72 h with and without the presence of PVA-90-12 hydrogel; the survival rate is determined by (B) crystal violet staining assay; and exhibited in (C). Only 1 mg/mL PVA-90-12 showed slight cytotoxic effect on RAW264.7 cells, as the survival rate was about 63.2%. Other concentrations showed no inhibitory effect on the growth of cells. It could be concluded that the PVA-9012 showed little cytotoxicity on RAW264.7 cells.

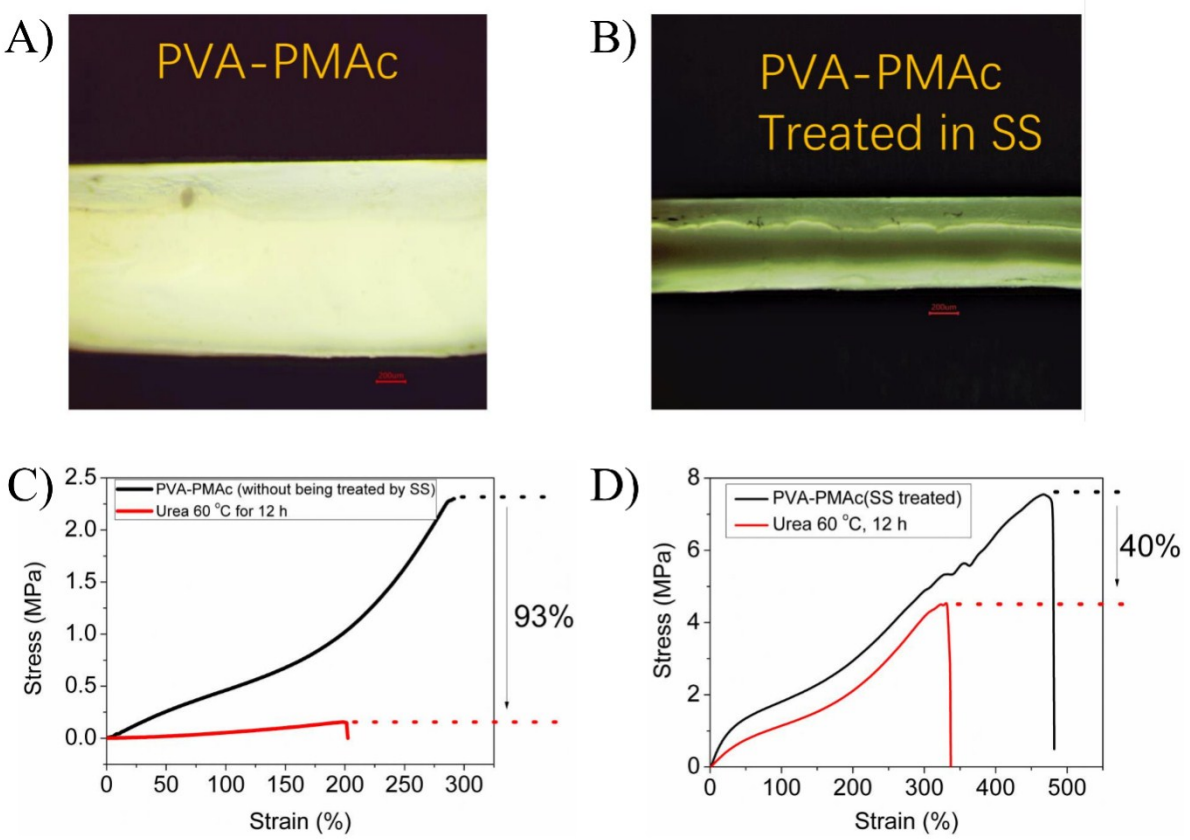

Figure S22. Photomicroscope of PVA-poly(methyl acrylic acid) (PMAc) composite hydrogel before and after soaking treatment in SS. Soaking treatment PVA-poly(methyl acrylic acid) (PMAc) composite hydrogel in SS significantly improve the stability of PMAc hydrogel. Upon soaking in urea at 60 °C for 12 h, the fracture stress of PVA-PMAc reduces by 93%, while PVA-PMAc treated by SS only reduces by 38%. Further optimization is still under progress.

References:

(1) Peppas, N. A.; Merrill, E. W. Poly(vinyl alcohol) hydrogels: Reinforcement of radiation-crosslinked networks by crystallization. *J. Polym. Sci.: Polym. Chem. Ed.* **1976**, 14, 441-457.

(2) G. M. Sapers. in The Produce Contamination Problem (Second Edition), Academic Press, San Diego, **2014**, pp. 389-431.

(3) Congdon, T.; Shaw, P.; Gibson, M. I. Thermoresponsive, well-defined, poly(vinyl alcohol) co-polymers. *Polym. Chem*. **2015**, 6, 4749-4757.

(4) Zhao, X. Multi-scale multi-mechanism design of tough hydrogels: building dissipation into stretchy networks. *Soft. Matter*. **2014**, 10, 672-687.

(5) Sun, T. L.; Luo, F.; Hong, W.; Cui, K.; Huang, Y.; Zhang, H. J.; King, D. R.; Kurokawa, T.; Nakajima, T.; Gong, J. P. Bulk Energy Dissipation Mechanism for the Fracture of Tough and Self-Healing Hydrogels *Macromolecule* **2017**, *50*, 2923-2931.

(6) Sun, J.Y.; Zhao, X.; Illeperuma, W. R. K.; Chaudhuri, O.; Oh, K. H.; Mooney, D. J.; Vlassak, J. J.; Suo, Z. Highly stretchable and tough hydrogels. *Nature*. **2012**, 489, 133-136.

(7) Zhang, H. J.; Sun, T. L.; Zhang, A. K.; Ikura, Y.; Nakajima, T.; Nonoyama, T.; Kurokawa, T.; Ito, O.; Ishitobi, H.; Gong, J. P. Tough Physical Double-Network Hydrogels Based on Amphiphilic Triblock Copolymers. *Adv. Mater.* **2016**, *28*, 4884-4890.

(8) Li, J.; Suo, Z.; Vlassak, J. J. Stiff, Strong, and Tough Hydrogels with Good Chemical Stability. *J. Mater. Chem. B* **2014**, 2, 6708-6713.

(9) Dai, X.; Zhang, Y.; Gao, L.; Bai, T.; Wang, W.; Cui, Y.; Liu, W. A Mechanically Strong, Highly Stable, Thermoplastic, and Self-Healable Supramolecular Polymer Hydrogel. *Adv. Mater.* **2015**, *27*, 3566-3577.

(10) Zhang, Y.; Li, Y.; Liu, W. Dipole–Dipole and H-Bonding Interactions Significantly Enhance the Multifaceted Mechanical Properties of Thermoresponsive Shape Memory Hydrogels. *Adv. Funct. Mater*. **2015**, 25, 471-480.

(11) Kamata, H.; Akagi, Y.; Kayasuga-Kariya, Y.; Chung, U.-i.; Sakai, T. "Nonswellable" Hydrogel Without Mechanical Hysteresis. *Science*. **2014**, 343, 873-875.

(12) Guo, H.; Sanson, N.; Hourdet, D.; Marcellan, A. Thermoresponsive Toughening with Crack Bifurcation in Phase-Separated Hydrogels under Isochoric Conditions. *Adv. Mater.* **2016**, *28*, 5857-5864.

(13) Yuan, N.; Xu, L.; Wang, H.; Fu, Y.; Zhang, Z.; Liu, L.; Wang, C.; Zhao, J.; Rong, J. Dual Physically Cross-Linked Double Network Hydrogels with High Mechanical Strength, Fatigue Resistance, Notch-Insensitivity, and Self-Healing Properties. *ACS Appl. Mater. & Inter.* **2016**, *8*, 34034-34044.

(14) Yavuz, M. S.; Cheng, Y.; chen, J.; Cobley, C. M.; Zhang, Q.; Rycenga, M.; Xie, J.; Kim, C.; Song, K, H.; Schwartz, A. G.; Wang, L. V.; Xia, Y. Gold nanocages covered by smart polymers for controlled release with near-infrared light. *Nat. Mater.* **2009**, *8*, 935-939.

(15) Calvert, P. Hydrogels for Soft Machines. *Adv. Mater*. **2009**, 21, 743-756.

(16) Guo, H.; Sanson, N.; Hourdet, D.; Marcellan, A. Thermoresponsive Toughening with Crack Bifurcation in Phase-Separated Hydrogels under Isochoric Conditions *Adv. Mater.* **2016**, *28*, 5857-5864.

(17) Sun, Y.; Xiang, N.; Jiang, X.; Hou, L. Preparation of high tough poly(vinyl alcohol) hydrogel by soaking in NaCl aqueous solution. *Mater. Lett*. **2017**, 194, 34-37.

(18) Yang, Y.; Wang, X.; Yang, F.; Shen, H.; Wu, D. A Universal Soaking Strategy to Convert Composite Hydrogels into Extremely Tough and Rapidly Recoverable Double-Network Hydrogels. *Adv. Mater*. **2016**, 28, 7178-7184.

(19) He, Q.; Huang, Y.; Wang, S. Hofmeister Effect-Assisted One Step Fabrication of Ductile and Strong Gelatin Hydrogels. *Adv. Funct. Mater*. **2018**, 28, 1705069.

(20) Zhao, D.; Huang, J. C.; Zhong, Y.; Li, K.; Zhang, L.; Cai, J. High-Strength and High-Toughness Double-Cross-Linked Cellulose Hydrogels: A New Strategy Using Sequential Chemical and Physical Cross-Linking. *Adv. Funct. Mater.* **2016**, *26*, 6279-6287.

(21) Xu, D.; Huang, J.; Zhao, D.; Ding, B.; Zhang, L. and Cai, J. High-Flexibility, High-Toughness Double-Cross-Linked Chitin Hydrogels by Sequential Chemical and Physical Cross-Linkings. *Adv. Mater.* **2016**, 28, 5844–5849.

(22) Yang, Y.; Wang, X.; Yang, F.; Wang, L.; Wu. D. C. Highly Elastic and Ultratough Hybrid Ionic–Covalent Hydrogels with Tunable Structures and Mechanics. *Adv. Mater.* **2018**, 30, 1707071.

(23) Ahmed, S.; Nakajima, T.; Kurokawa, T.; Anamul Haque, M.; Gong, J. P. *Polymer* **2014**, *55*, 914-923.

(24) Wang, S.; Guo, G.; Lu, X.; Ji, S.; Tan, G.; Gao, L. Facile Soaking Strategy towards Simultaneously Enhanced Conductivity and Toughness of Self-Healing Composite Hydrogels through Constructing Multiple Noncovalent Interactions. *ACS Appl. Mater. & Inter.* **2018,** 10, 19133-19142.

(25) Hassan, C. M.; Peppas, N. A. Structure and Morphology of Freeze/Thawed PVA Hydrogels. *Macromolecule*. **2000**, 33, 2472-2479.

(26) Xu, L.; Zhao, X.; Xu, C.; Kotov, N. A. Water-Rich Biomimetic Composites with Abiotic Self-Organizing Nanofiber Network. *Adv*. *Mater*. **2018**, 30, 1703343.